

NEUTRINO NUCLEUS SCATTERING

PETR VOGEL

*Physics Department 161-33, California Institute of Technology, Pasadena,
California 91125*

E-mail: vogel@lamppost.caltech.edu

The status of the theoretical description of the neutrino-nuclear interaction for low and intermediate energies is reviewed and its results are compared with the existing data. Particular emphasis is on ^{12}C , the ingredient of liquid scintillator, and on ^{16}O , the main component of the water Čerenkov detectors. First, I show that the data on the exclusive process populating the ground state of ^{12}N are well reproduced by the theory. This is also the case for the excitation of the continuum with low energy neutrinos from the muon decay at rest and for muon capture. However, for not yet understood reasons, the theory overestimates the cross section for higher energy neutrinos from the pion decay in flight, by up to 50%. I also show that the Continuum Random Phase Approximation and the Relativistic Fermi Gas model give very similar full and differential cross sections for neutrino energies of several hundred MeV, thus checking one method against the other.

1 Introduction and summary

The observation of neutrinos and antineutrinos is often based on their interaction with complex nuclei. The study of the corresponding neutrino-nuclear cross section is rarely the primary motivation of these experiments; their aim most often belongs to the category of “fundamental processes”, e.g., one tries to deduce from the outcome either the properties of neutrinos themselves (as in the searches for neutrino oscillations) or of the sources of the neutrinos (as in the attempts to observe neutrinos from supernovae).

Neutrino-nuclear scattering is, therefore, for most people just a tool; it belongs to “neutrino engineering”^a. As with all tools, a solid understanding of cross sections in neutrino-induced reactions, particularly on light nuclei, is a necessity. This includes especially ^{12}C , an ingredient of liquid scintillators, and ^{16}O , the basic component of water Čerenkov detectors.

There are numerous examples of application of nuclear targets. Let me enumerate some of them, with brief comments:

- Detection of solar neutrinos. This involves ν_e of the lowest energies in comparison with essentially all other applications. When nuclear targets

^aI believe that this, slightly derogatory but nevertheless rather accurate term was coined by G. T. Garvey.

are used (chlorine, gallium, iodine, etc.) usually bound discrete final states are populated.

- Signal in the KARMEN and LSND detectors. The sources involve somewhat higher energy neutrinos (e.g. from the pion and muon decays at rest). The target is liquid scintillator containing hydrogen and ^{12}C nuclei. As I will describe in more detail later, neutrinos excite both the discrete bound states and the continuum final states.
- Detection of atmospheric neutrinos. Here the energies are substantially higher. In most applications the target nuclei are ^{16}O (water Čerenkov detectors). Essentially all final states are in the continuum. Details of nuclear structure play a secondary, but still nonnegligible role.
- r-process nucleosynthesis. There, neutrinos of all flavors and moderate energies are expected to interact with nuclei far from stability. Both discrete and continuum final states are important. This application of the neutrino-nuclear interaction is based, at present, only on theoretical estimates of the corresponding cross sections.
- Detection of supernova ν_μ and ν_τ . These neutrinos will interact only through the neutral current, and can be detected by e.g. observation of the deexcitation of ^{16}O in water Čerenkov detectors. Again, the corresponding cross section is based only on theoretical estimates.

Since only a few of the just enumerated cross sections have been measured, one has to rely often on nuclear theory for their evaluation. The description of the theoretical effort, and comparison with existing data, are the topics of this talk.

Ideally, one would like to have a relatively simple universal recipe valid for all nuclei and all neutrino energies. Alas, but perhaps not surprisingly, my main message is that such a recipe does not exist. Instead, for each energy one needs a somewhat different approach. These approaches then should smoothly connect at the corresponding boundaries of applicability.

- At the lowest energies the details of nuclear structure, i.e., all the complications related to the many-body nature of the nuclear system, really matter. The nuclear *shell model* is then the method of choice.
- At intermediate energies the shell model becomes untractable (or essentially so). At the same time, the particle-hole nature of the final nuclear state becomes the most important feature. Some form of the *Random Phase Approximation* (RPA) is then the method of choice.

- At yet higher energies, the details of the nucleon-nucleon interaction become less important. The *Fermi gas model* is then the method of choice.

In the following I will concentrate on the neutrino- ^{12}C interaction where a number of experimental results exist. These include measurements of charged-current reactions induced by both electron-^{1,2} and muon-neutrinos², exciting both the ground and continuum states in ^{12}N . The inclusive cross section for $^{12}\text{C}(\nu_e, e)^{12}\text{N}^*$ ^{1,2,3}, agrees well with calculations. By contrast, there is a discrepancy between calculations^{4,5,6,7} (with some notable exceptions^{8,9}) and the measured² inclusive cross section for $^{12}\text{C}(\nu_\mu, \mu)^{12}\text{N}^*$, which uses higher energy neutrinos from pion decay-in-flight. The disagreement is disturbing in light of the simplicity of the reaction and in view of the fact that parameter-free calculations, such as those in^{4,5}, describe well other weak processes governed by the same weak current nuclear matrix elements. The exclusive reactions populating the ground state of the final nucleus, $^{12}\text{C}(\nu_e, e)^{12}\text{N}_{gs}$ and $^{12}\text{C}(\nu_\mu, \mu)^{12}\text{N}_{gs}$, and the neutral current reaction $^{12}\text{C}(\nu_e, \nu'_e)^{12}\text{C}(15.11 \text{ MeV})$ have been measured^{1,2} as well, and agree perfectly with theoretical expectations.

My own theoretical work, which I will review below, is based on a series of calculations performed in collaboration with Edwin Kolbe, Karlheinz Langanke and Jonathan Engel.

2 Exclusive Reactions

Among the states in the final nucleus ^{12}N , which is populated by the charged current reactions with beams of ν_e or ν_μ , the ground state $I^\pi = 1^+$ plays a special role. It is the only bound state in ^{12}N , and can be recognized by its positron decay ($T_{1/2} = 11 \text{ ms}$) back to ^{12}C . Moreover, the analog of the $^{12}\text{N}_{gs}$, the $I^\pi = 1^+$ state with isospin $T = 1$ at 15.11 MeV in ^{12}C , can be populated by the neutral current neutrino scattering, and is recognizable by its emission of the 15.11 MeV photon. Finally, even though there are several bound states in ^{12}B , its ground state, the analog of the other two $I^\pi T = 1^+1$ states, is the state most strongly populated in muon capture on ^{12}C . Again, the population of the bound states in ^{12}B can be separated from the continuum by observing its electron decay ($T_{1/2} = 20.2 \text{ ms}$).

Theoretical evaluation of the exclusive cross sections is constrained by the obvious requirement that the same method, and the same parameters, must also describe the related processes, shown schematically in Fig. 1. It turns out that this requirement essentially determines the neutrino induced cross section for the energies of present interest. It does not matter which method of calculation is used, as long as the constraints are obeyed.

Table 1: Comparison of calculated and measured cross sections, in units of 10^{-42}cm^{-2} and averaged over the corresponding neutrino spectra, for the neutrino induced transitions $^{12}\text{C}_{gs} \rightarrow ^{12}\text{N}_{gs}$ and $^{12}\text{C}_{gs} \rightarrow ^{12}\text{C}(15.11 \text{ MeV})$. For the decay at rest the ν_e spectrum is normalized from $E_\nu = 0$, while for the decay in flight the ν_μ and $\bar{\nu}_\mu$ spectra are normalized from the corresponding threshold. See the text for explanations.

	$^{12}\text{C}(\nu_e, e^-)^{12}\text{N}_{gs}$ decay at rest	$^{12}\text{C}(\nu_\mu, \mu^-)^{12}\text{N}_{gs}$ decay in flight	$^{12}\text{C}(\nu, \nu')^{12}\text{C}(15.11)$ decay at rest
experiment ¹	$9.4 \pm 0.5 \pm 0.8$	-	$11 \pm 0.85 \pm 1.0$
experiment ²	$9.1 \pm 0.4 \pm 0.9$	$66 \pm 10 \pm 10$	-
experiment ³	$10.5 \pm 1.0 \pm 1.0$	-	-
Shell model ¹⁰	9.1	63.5	9.8
CRPA ^{4,5}	8.9	63.0	10.5
EPT ¹¹	9.2	59	9.9

The comparison between the measured and calculated values is shown in Table 1. There, three rather different methods of calculation were used, all giving excellent agreement with the data.

The first approach is a restricted shell-model calculation. Assuming that all structure in the considered low-lying states is generated by the “valence” nucleons in the p -shell, there are only four one-body densities (OBD) which fully describe all necessary nuclear matrix elements. The most straightforward way of obtaining the OBD is by diagonalizing a thoroughly tested residual interaction. However, the resulting p -shell OBD do not describe the processes in Fig. 1 very well; to remedy this one can modify the one-body densities (ad hoc) in such a way that all these “auxiliary” data are correctly reproduced. This then gives the results listed in line 4 of Table 1.

Effects of configurations beyond the p shell might explain the need for the renormalization of the one-body densities produced by a reasonable p -shell Hamiltonian. We therefore also calculate the rates of all the reactions above, including exclusive neutrino capture, in the Random Phase Approximation (RPA), which does include multishell correlations, while treating the configuration mixing within the p shell only crudely. Again an adjustment is needed (a “quenching” of all matrix elements by an universal, but substantial, factor 0.515). However, the neutrino cross sections in line 5 of Table 1 agree with the measurements perfectly.

The third approach is the “elementary-particle treatment” (EPT). Instead of describing nuclei in terms of nucleons, the EPT considers them elementary

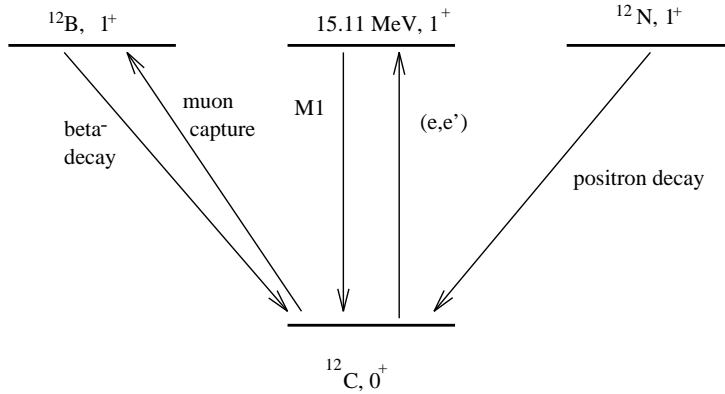


Figure 1: Constraints on the exclusive channels.

and describes transition matrix elements in terms of *nuclear* form factors deduced from experimental data. The EPT approach was extended in Ref. ¹⁰ to the higher neutrino energies relevant to the LSND decay-in-flight ν_μ 's by appropriately including the lepton mass.

An example of the energy dependence of the exclusive cross section is shown in Fig. 2 for the ν_μ induced exclusive reaction. As one can see, the cross section raises sharply from its threshold ($E_{thr} = 123 \text{ MeV}$) and soon reaches its saturation value, i.e., it becomes almost energy independent. This means that the yield of the $^{12}\text{C} + \nu_\mu$ reaction essentially measures just the flux normalization above the reaction threshold. At the same time, the yield is insensitive to the energy distribution of the muon neutrinos in the beam.

3 Inclusive Reactions

The inclusive reactions $^{12}\text{C}(\nu_e, e)^{12}\text{N}^*$, with ν_e neutrinos from the muon decay-at-rest and $^{12}\text{C}(\nu_\mu, \mu)^{12}\text{N}^*$ with the higher energy ν_μ neutrinos from the pion decay-in-flight populate not only the ground state of ^{12}N but also the continuum states. The corresponding cross sections involve folding over the incoming neutrino spectra and integrating over the excitation energies in the final nucleus. By convention, we shall use the term “inclusive” for the cross section populating only the continuum (i.e., without the exclusive channel) for $^{12}\text{C}(\nu_e, e)^{12}\text{N}^*$ with the decay-at-rest ν_e , while for the reaction $^{12}\text{C}(\nu_\mu, \mu)^{12}\text{N}^*$ with the decay-in-flight ν_μ the term is used for the total cross section (the exclusive channel then represents only a small fraction of the total).

Muon capture, $^{12}\text{C}(\mu, \nu_\mu)^{12}\text{B}^*$, belongs also to this category. It involves

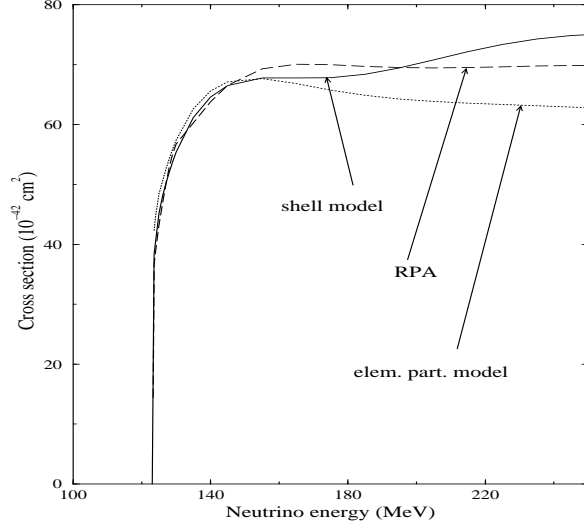


Figure 2: Energy dependence of the cross section for the reaction $^{12}\text{C} + \nu_{\mu} \rightarrow ^{12}\text{N}_{g.s} + \mu^{-}$.

momentum transfer of $q \approx m_{\mu}$, intermediate between the two neutrino capture reactions above. Since ^{12}B and ^{12}N are mirror nuclei, all three reactions should be considered together. In this case again the term “inclusive” will be used only for the part of the rate populating the continuum in ^{12}B .

What theoretical approach should one use in order to describe such reactions? One possibility is to use the continuum random phase approximation (CRPA). The method has been used successfully in the evaluation of the nuclear response to weak and electromagnetic probes¹². In particular, we have tested it, with good agreement, in the calculation of the inelastic electron scattering¹³ on ^{12}C involving very similar excitation energies and momentum transfers as the weak processes of interest. As an example I show in Fig. 3 the comparison of the experimental data and the results of the CRPA for the inclusive electron scattering¹⁴. One can see that CRPA describes quite well both the magnitude and shape of this cross section over the entire range of excitation energies and momentum transfers.

For muon capture the CRPA¹⁵ gives the inclusive rates of 0.342, 0.969, and $26.2 \times 10^5 \text{ s}^{-1}$ for ^{12}C , ^{16}O and ^{40}Ca ; to be compared with the measured rates of 0.320, 0.924, and $25.6 \times 10^5 \text{ s}^{-1}$ for the same nuclei. This good agreement is

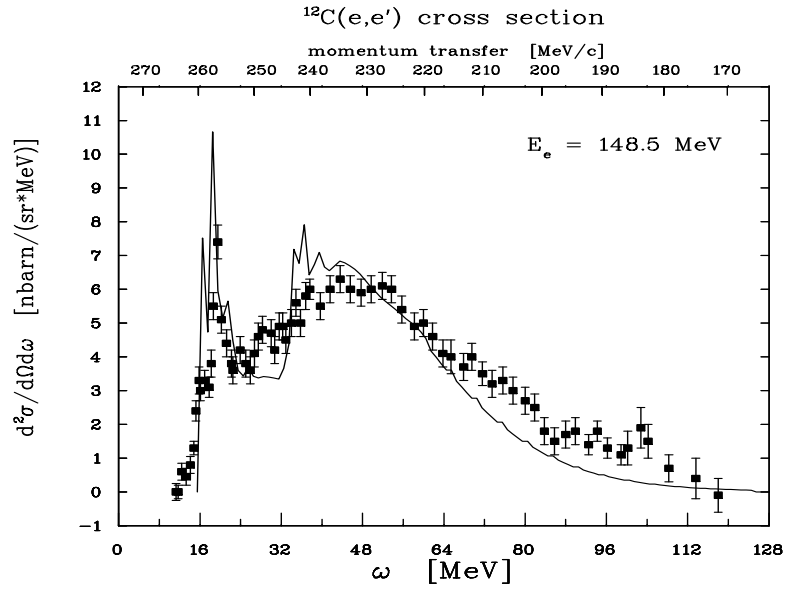


Figure 3: Data (points with error bars) and calculated cross section for the inclusive electron scattering on ^{12}C as a function of the excitation energy ω . The corresponding momentum transfer is displayed on the upper scale.

again obtained without any parameter adjustment. In particular, as discussed in Ref.¹⁵, no renormalization of the axial vector coupling constant g_A in nuclear medium is required.

Can one understand why CRPA is apparently able to describe the inclusive processes without the need for parameter adjustment, unlike the case of the exclusive reactions discussed earlier? Another way of thinking about this problem is the question to what extent the correlations of nucleons within the nuclear p shell influence the result. In order to shed light on this, one can evaluate the total strength of various operators \hat{O} , i.e. the norm of the vector $\hat{O}|g.s.\rangle$, with and without the effect of the correlations. Note that the total strength depends only on the ground state wave function and is therefore relatively easy to evaluate. For the positive parity operators this is done in Table 2.

Table 2: The full strength within the nuclear p shell evaluated for the operators in column 1. The SM column is the exact shell model strength calculated with the Cohen-Kurath interaction. The “naive” column corresponds to the $(1p_{3/2})^8$ configuration, i.e. no correlations whatsoever. In the last column the strength for transitions with $2\hbar\omega$ excitation energy is shown for comparison.

Operator	SM	“naive”	$2\hbar\omega$
GT($\sigma\tau$)	1.51	8.00	0.00
$r^2 Y_2$	1.37	1.98	9.95
$r^2 (Y_2 s)^{I=1}$	0.11	0.08	-
$r^2 (Y_2 s)^{I=2}$	0.33	0.75	-
$r^2 (Y_2 s)^{I=3}$	0.20	0.00	-
$\sum_{\lambda} r^2 (Y_2 s)^{I=\lambda}$	0.63	0.83	7.47

Table 2 illustrates the well known fact that the p shell correlations are very important for the Gamow-Teller operator $\sigma\tau$. (Note that RPA gives the total GT strength of 5.5, only slightly reduced when compared to the “naive” estimate. Also, the exact shell model predicts that a strength of 0.12 goes to excited 1^+ states, which are absent when the naive model is considered.)

But the situation with quadrupole operators is rather different. The total p shell strength of the spin-independent operator, and the strength summed over the multipolarities of the spin-dependent operators is affected by the correlations only at the level of 30-40%, even though the individual spin dependent multipoles are affected more. Moreover, the p shell strength represents only a small fraction of the total quadrupole strength, which is concentrated in the $2\hbar\omega$ excitations, unaffected by correlations as long as we assume that the

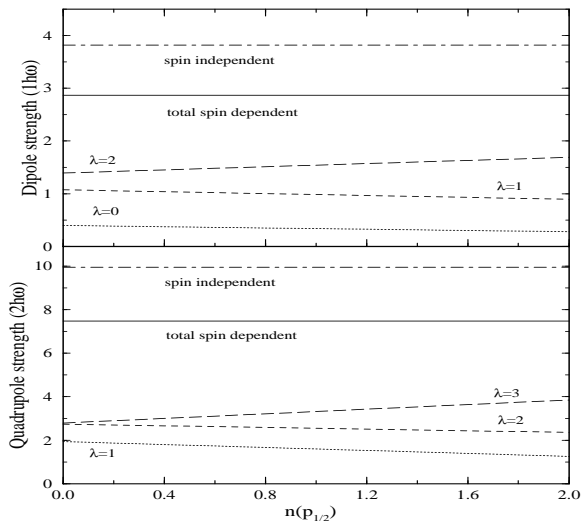


Figure 4: Total strength of the dipole (upper part) and quadrupole (lower part) operators versus the occupation of the $p_{1/2}$ subshell. The curves are labelled by the corresponding angular momentum of the $r^l(Y_{ls})^{I=\lambda}$ operators for $l = 1$ and $l = 2$.

ground state has only p shell nucleons.

However, the inclusive reactions we are considering are dominated by the excitations of the negative parity states. To what extent does the strength depend on the occupation of the $p_{1/2}$ subshell? Note that Auerbach et al.⁹ claim that when there are about 1.6 nucleons in the $p_{1/2}$ subshell, the inclusive cross section is reduced substantially. In order to test the sensitivity to this “pairing” effect, we plot in Fig. 4 the dipole and quadrupole strengths as a function of the $p_{1/2}$ subshell occupation. We find that when summed over multipoles the strength is totally independent of this occupation number. But even the individual multipoles depend on the occupation numbers only mildly. Thus, at least for the full strength, we find again that p shell correlations are relatively unimportant.

What are the momentum transfers and excitation energies involved in the inclusive reactions which we would like to describe? For the $^{12}\text{C}(\nu_e, e)^{12}\text{N}^*$ with the electron neutrinos originating in the muon decay at rest, the typical momentum transfer is $\langle|\vec{q}|\rangle \simeq 50$ MeV, and the typical excitation energy is $\omega \simeq 20$ MeV. For the inclusive muon capture $^{12}\text{C}(\mu^-, \nu_\mu)^{12}\text{B}^*$ we have $\langle|\vec{q}|\rangle \simeq 90$ MeV and the typical excitation energy is $\omega \simeq 25$ MeV. Finally for the $^{12}\text{C}(\nu_\mu, \mu^-)^{12}\text{N}^*$ with the muon neutrinos originating in the pion decay in

flight at LAMPF we have $\langle |\vec{q}| \rangle \simeq 200$ MeV and the typical excitation energy is $\omega \simeq 40$ MeV. The excitation energies should be compared with the nuclear shell spacing $\hbar\omega \simeq 41/A^{1/3}$ MeV, which for ^{12}C is equal to about 18 MeV. Thus, in order to describe all the above inclusive processes in the framework of the nuclear shell model, one would have to include fully and consistently at least all $2\hbar\omega$ excitations, and possibly even the $3\hbar\omega$ ones. That is not impossible, but represents a formidable task. On the other hand, CRPA can easily handle such configuration spaces. Moreover, it properly describes the continuum nature of the final nucleus. Finally, as argued above, the crudeness with which the correlations of the p shell nucleons is treated in the CRPA is expected to be relatively unimportant.

For the inclusive reaction $^{12}\text{C}(\nu_e, e^-)^{12}\text{N}^*$, with ν_e neutrinos from the muon decay-at-rest the calculation gives⁴ the cross section of 6.3×10^{-42} cm² using the Bonn potential based G-matrix as the residual interaction, and 5.9×10^{-42} cm² with the schematic Migdal force. (The two different residual interactions are used so that one can estimate the uncertainty associated with this aspect of the problem.) Both are clearly compatible with the measured values of $6.4 \pm 1.45[\text{stat}] \pm 1.4[\text{syst}] \times 10^{-42}$ cm² by the Karmen collaboration¹ (the more recent result gives somewhat smaller value $5.1 \pm 0.6 \pm 0.5^{16}$) and with $5.7 \pm 0.6[\text{stat}] \pm 0.6[\text{syst}] \times 10^{-42}$ cm² obtained by the LSND collaboration². If one wants to disregard the error bars (naturally, one should not do that), one can average the two calculated values as well as the two most recent measurements and perhaps conclude that the CRPA calculation seems to exceed the measured values by about 10-15%. A similar tendency can be found, again with some degree of imagination, in the comparison of the muon capture rates discussed earlier.

So far we have found that CRPA describes the inclusive reactions quite well. Other theoretical calculations, e.g.^{7,9} describe these reactions with equal success. This is no longer the case when we consider the reaction $^{12}\text{C}(\nu_\mu, \mu)^{12}\text{N}^*$ with the higher energy ν_μ neutrinos from the pion decay-in-flight. This reaction involves larger momentum transfers and populates states higher up in the continuum of ^{12}N . Our calculation^{4,5} gives the cross section of 19.2×10^{-40} cm², considerably larger than the measured² value of $11.3 \pm 0.3[\text{stat}] \pm 1.8[\text{syst}]$ in the same units. The origin of the discrepancy is not clear, but as stressed in the discussion of the exclusive reaction, the ν_μ flux normalization is not a likely culprit. While Ref.⁶ confirms our result, Ref.⁸ gets a value close to the experiment by using a generalization of the EPT approach. It is questionable, however, that the assumptions used in⁸ are justified¹⁴.

Other recent theoretical calculations span the region between the CRPA and experiment. So, Singh et al.⁷ give $16.65 \pm 1.37 \times 10^{-40}$ cm², clearly higher

than the experiment but somewhat lower than the CRPA. On the other hand, Ref.⁹ gives 13.5 - 15.2 in the same units, value which is even closer to the experiment. The main difference in that work is the inclusion of pairing, which as I argued above, should not represent a substantial effect.

This discrepancy has been with us for quite some time now. A small, but not insignificant step which removes part of it is the new simulation of the ν_μ flux for the decay-in-flight beam (R. Imlay, private communication). As I emphasized above, the exclusive reaction fixes to some extent the flux normalization, but is insensitive to its shape. The revision, which is within the error bars of the previous flux, results in moving the most probable measured value up from 11.2 to 12.4 (subject to revision and with as yet undetermined error bars). At the same time, the CRPA calculated value moves down from 19.3 to 18.0 (all in 10^{-40} cm^2). While diminished, the discrepancy is still clearly present, and also clearly exceeds the 10-15% perhaps suggested by the lower energy inclusive reactions discussed above. It would be very important to perform a large scale shell model calculation, including up to $3\hbar\omega$ excitations, to put the matter to rest.

The importance of the inclusive $^{12}\text{C}(\nu_\mu, \mu^-)^{12}\text{N}^*$ reaction goes beyond its significance for testing our ability to perform calculations of this kind. The LSND collaboration announced evidence for $\nu_\mu \rightarrow \nu_e$ oscillations based on the same ν_μ neutrino beam from the pion decay in flight¹⁷. The resulting electron neutrinos ν_e are detected by their charged current interaction with the ^{12}C nuclei, and are recognized by the observation of high energy (60 - 200 MeV) electrons. In order to extract the oscillation probability from the observed number of events, however, one has to know the corresponding inclusive cross section, analog of which is the discrepant result just discussed.

One has to remember, however, that the ν_μ induced reaction has a threshold of 123 MeV, while the ν_e induced reaction has a threshold of only 17 MeV (or with the experimental constraint on the electron energy the effective threshold is about 80 MeV). At the same time the decay-in-flight neutrino beam is essentially monotonically decreasing with the neutrino energy. Consequently the neutrino energies involved in the ν_e induced reaction will be smaller than in the ν_μ induced reaction. This is illustrated in Fig. 5 where cross sections for both reactions are compared in the upper panel. In the lower panel, assuming full conversion $\nu_\mu \rightarrow \nu_e$, I plot the cross section \times neutrino flux (i.e. the number of events) as a function of the neutrino energy. One can clearly see that the oscillation signal would be caused by neutrinos of lower energy on average than the neutrinos involved in the inclusive $^{12}\text{C}(\nu_\mu, \mu^-)^{12}\text{N}^*$ reaction. While this does not guarantee that the uncertainty in the cross section will be lower, it makes this assumption rather plausible.

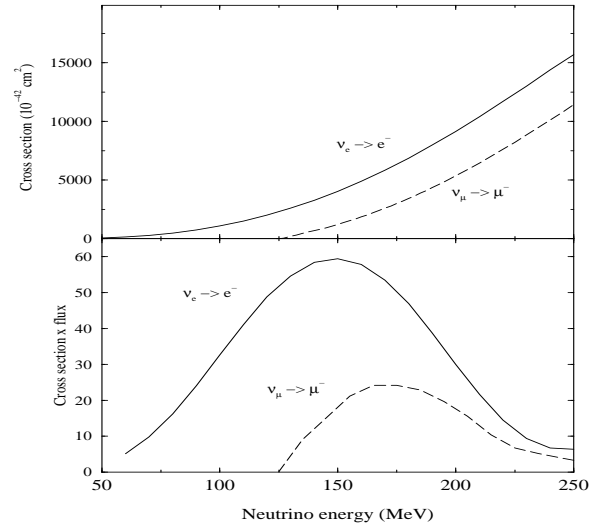


Figure 5: The cross sections for indicated reactions on ^{12}C are compared in the lower panel, while in the upper panel the cross section is multiplied by the corresponding decay-in-flight flux.

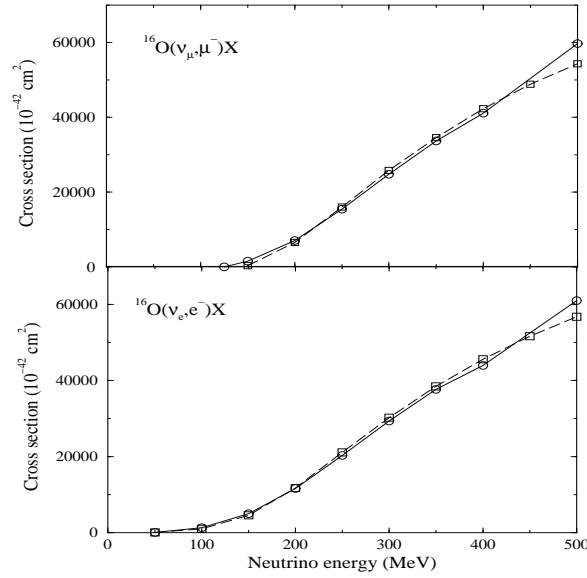


Figure 6: The cross sections for indicated reactions on ^{16}O in units of 10^{-42} cm^2 . The dashed line is for the relativistic Fermi gas method and the full line is for the continuum random phase approximation (CRPA).

4 Angular distribution: CRPA versus Fermi gas model

We now turn our attention to the neutrino induced reactions at higher energies, closer to those encountered in the study of atmospheric neutrinos. As we stressed earlier, at sufficiently high neutrino energy the description using the CRPA method and the relativistic Fermi gas (RFG) should give identical, or at least very similar results. Here we would like to compare the two methods not only as far as the full cross section is concerned, but also for the description of the angular distribution of the emitted lepton. We use the Smith and Moniz formulation of the RFG method¹⁸. Earlier, the CRPA has been applied to the atmospheric neutrino problem in Ref.¹⁹.

The application of CRPA to the angular distribution in the neutrino induced reactions was developed by Kolbe²⁰ who applied it to the charged current reactions on ^{12}C relevant to the LSND experiment. A satisfactory agreement with the experimental distributions was obtained. The results presented here were also obtained by Kolbe and will be reported on in detail elsewhere.

In Fig. 6 I show the total cross section for the charged current reactions

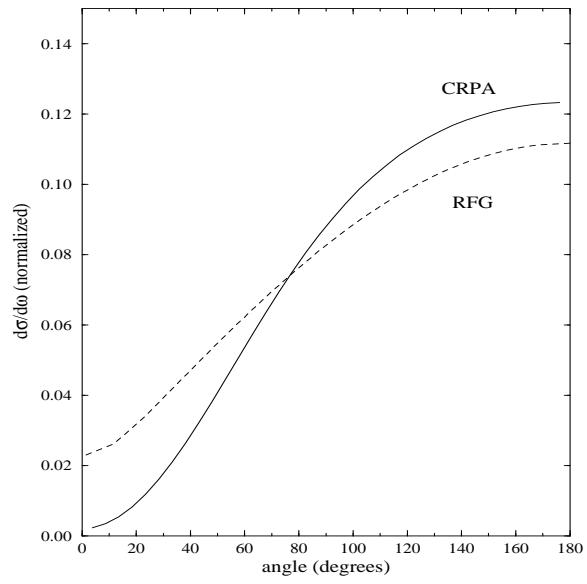


Figure 7: The differential cross sections for the reaction $^{16}\text{O}(\nu_e, e^-)X$ for the neutrino energy $E_\nu = 100$ MeV. The dashed line is for the relativistic Fermi gas method and the full line is for the continuum random phase approximation (CRPA).

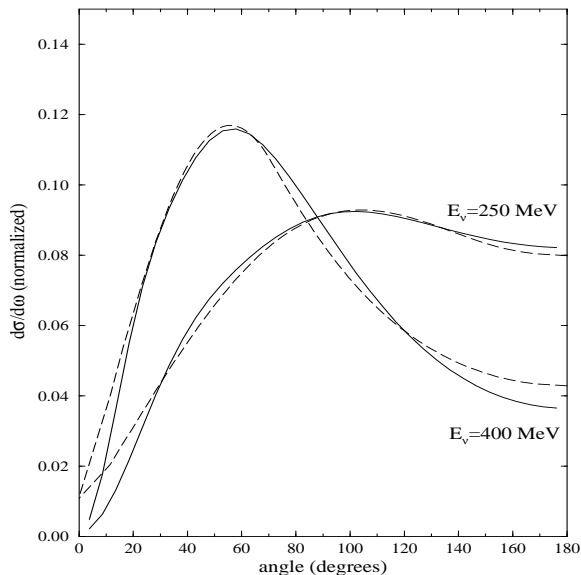


Figure 8: The differential cross sections for the reaction $^{16}\text{O}(\nu_e, e^-)X$ for the neutrino energies of $E_\nu = 250$ and 400 MeV. The dashed line is for the relativistic Fermi gas method and the full line is for the continuum random phase approximation (CRPA).

on ^{16}O calculated by both methods for neutrino energies up to 500 MeV. One can see that over that energy interval the two methods agree quite well. (The RFG was evaluated with the standard values $p_f = 225$ MeV and $e_b = 27$ MeV deduced from the electron-nucleus scattering data²¹.)

The problem of the angular distribution is very important these days. The Super-Kamiokande collaboration reported evidence for oscillation of atmospheric neutrinos²². The data show a zenith angle dependence of the muon neutrino deficit for both the sub-GeV and multi-GeV samples. Of particular interest for the present work is the observation that the muons are essentially isotropic for momenta $p < 400$ MeV, and show a zenith angle anisotropy at higher momenta.

Of course, the observed direction in Super-Kamiokande is the direction of the muon or electron. The direction of the neutrino is then deduced from the expected angular correlation in the neutrino - oxygen quasi-elastic charged current reaction. The analysis in Ref.²² is based on RFG. How good is that for neutrino energies of a few hundred MeV?

First, as pointed out by Kolbe²⁰ at energies corresponding to the neutrino

beams available at LAMPF in both the $^{12}\text{C}(\nu_\mu, \mu^-)^{12}\text{N}^*$ and $^{12}\text{C}(\nu_e, e^-)^{12}\text{N}^*$ reactions the muons and electrons are in fact backward peaked. This is also true for the charged current reactions on ^{16}O as shown in Fig. 7. There one can see that both methods predict backward peaking which is considerably more pronounced in CRPA than in the RFG method.

In Fig.8 I compare the differential cross section for the two methods for neutrino energies of 250 and 400 MeV. I use here electrons as outgoing leptons so that the outgoing particle is fully relativistic, and the threshold effects are negligible. One can see in Fig. 8 that, first of all, at these energies the two methods give essentially identical results, as expected. Also, the peak in angular distribution is gradually shifting to forward angles. That is again in at least qualitative agreement with the Super-Kamiokande finding where very little asymmetry was found for muons with momenta less than 400 MeV.

The results of this Section thus serve two purposes. First, they show that at energies of several hundred MeV the continuum random phase approximation (CRPA), and the relativistic Fermi gas (RFG) model give essentially identical results both for the full and differential cross sections. Let me stress that both calculations are parameter free, in the sense that the parameters involved were obtained independently, not adjusted for the weak processes in question. The second lesson, related to the first one, is an indirect confirmation of the procedure used to analyze the zenith angle dependence of the atmospheric neutrino anomaly.

5 Yet higher energies

In this section I would like to report on a piece of “work in progress”. So far, I have shown that at the lowest energies, corresponding to the muon decay-at-rest neutrinos, various methods including the CRPA and the nuclear shell model, give very similar results. This then tests the one method against the other. Also, at those low neutrino energies, the *absolute* cross sections are correctly reproduced.

Next came the discussion of the inclusive reactions using the pion decay-in-flight ν_μ of somewhat higher energy. There, unfortunately, reliable shell model calculations are not available yet. At the same time, the CRPA overestimates the measured cross section by about a factor 1.5. Even though various theoretical papers come a bit closer to the experiment, those calculations have not been so thoroughly tested as the CRPA. In any case, a majority of these results also gives cross sections which are larger than the measured one. The reasons for this discrepancy remain unclear. However, it is possible that the problem lies in our ability to describe the neutrino-nucleus interaction at these

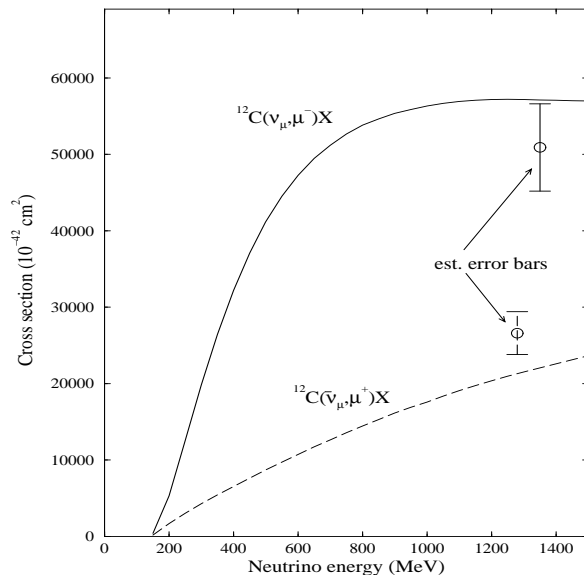


Figure 9: Cross sections for the indicated reactions calculated using the RFG model with parameters determined from the quasielastic electron scattering ($e_F = 221$ MeV, $e_b = 25$ MeV). The Brookhaven AGS data with estimated error bars, and for an average energy, are shown for comparison.

energies.

Next, in the previous section, I have shown that at energies of several hundred MeV the CRPA and RFG give essentially identical total and differential cross sections. The obvious experimental data at these energies come from the study of atmospheric neutrinos, and are subject to the uncertainties associated with the incoming flux of the atmospheric neutrinos. Thus it is difficult to make a model independent comparison between the calculated and measured absolute cross sections.

However, at yet higher energies, of about 1 GeV, the cross section for ν_μ and $\bar{\nu}_\mu$ has been measured in a series of experiment at the Brookhaven AGS in the early eighties (see e.g. ^{23,24}). These experiments, among other things, allowed the determination of the axial vector form factor of the nucleon. The detector used at AGS was a liquid scintillator based detector²⁵; the cross section, measured for both ν_μ and $\bar{\nu}_\mu$ beams thus represent the quantity we have been discussing all along, namely the cross section for the neutrino- ^{12}C quasielastic scattering. Thus it is tempting to extend the RFG model calcula-

tion to the corresponding energies, and compare the calculated and measured cross sections. One would be able to see in that way whether the agreement is restored again at these energies where nuclear structure presumably plays relatively minor role.

The problem is the extraction of the absolute cross section from the published data. The quasielastic scattering cross section was used in the experiment to verify the Monte-Carlo simulation of the beam. From the consistency of the measured and expected rates it is obvious that the modeling of the beam was correct, but it would be desirable to make this statement more quantitative. This is the part of the analysis that remains to be done.

The preliminary comparison is presented in Fig. 9 for both beams. The experimental error bars are just estimates, as explained above. Also, the wide band beam is replaced by a beam with single average energy. (That is not too critical at this stage, since the cross section almost saturates at the considered energies.) With all these caveats, Fig. 9 shows that the RFG describes the data to accuracy not worse than about 20%, and likely much better. Whatever is causing the discrepancy at the LAMPF energies has healed itself, as expected, at these much higher energies.

Acknowledgments

It is my pleasant duty to thank my collaborators, Jon Engel, Karlheinz Langanke, and especially Edwin Kolbe. I have also benefited from discussions with members of the LSND collaboration, in particular with R. Imlay, W. Louis, and D. H. White who inspired me to consider the higher energy extension of the present calculation. This work was supported by the US Department of Energy under Grant No. DE-FG03-88ER-40397.

References

1. G. Drexlin et al., KARMEN collaboration, Phys. Lett. **B267** (1991) 321.
B. Zeitnitz, KARMEN Collaboration, Prog. Part. Nucl. Phys. **32**, (1994) 351-373.
J. Kleinfeler et al. KARMEN collaboration, in *Neutrino'96*, eds. K. Enquist, K. Huitu, and J. Maalampi, World Scientific, Singapore, 1997.
2. M. Albert et al., Phys. Rev. **C51**, 1065 (1995).
C. Athanassopoulos et al., Phys. Rev. C **55**, 2078 (1997).
C. Athanassopoulos et al., Phys. Rev. C **56**, 2806 (1997).
R. Imlay, Nucl. Phys. **A629**, 531c (1998).
3. D.A. Krakauer et al., Phys. Rev. **C45**, 2450 (1992).

4. E. Kolbe, K. Langanke, and S. Krewald, Phys. Rev. **C49**, (1994) 1122.
5. E. Kolbe, K. Langanke, F.-K. Thielemann, and P. Vogel, Phys. Rev. **C52**, 3437 (1995).
6. T. S. Kosmas and E. Oset, Phys. Rev. C **53**, 1409 (1996).
7. S. K. Singh, N. C. Mukhopadhyay, and E. Oset, Phys. Rev. C **57**, 2687 (1998).
8. S. L. Mintz and M. Pourkaviani, Nucl. Phys. **A594**, 346 (1995).
9. N. Auerbach, N. Van Giai, and O. K. Vorov, Phys. Rev. C **56**, R2368 (1997).
10. J. Engel, E. Kolbe, K. Langanke, and P. Vogel, Phys. Rev. **C54**, 2740 (1996).
11. M. Fukugita, Y. Kohyama and K. Kubodera, Phys. Lett. **B212**, 139 (1988).
12. M. Buballa, S. Drożdż, S. Krewald, and J. Speth, Ann. Phys. (N.Y.) **208**, 346 (1991).
13. J. E. Leiss and R. E. Taylor, as quoted in W. Czyz, Phys. Rev. **131**, 2141 (1963).
14. E. Kolbe, K. Langanke, and P. Vogel, Nucl. Phys. **A613**, 382 (1997).
15. E. Kolbe, K. Langanke and P. Vogel, Phys. Rev. **C50**, 2576 (1994).
16. R. Maschuw et al., Prog. Part. Nucl. Phys. **40**, 183 (1998).
17. C. Athanassopoulos et al., Phys. Rev. Lett. **81**, 1774 (1998).
18. R. A. Smith and E. J. Moniz, Nucl. Phys. **B43**, 605 (1972).
19. J. Engel, E. Kolbe, K. Langanke, and P. Vogel, Phys. Rev. D **48**, 3048 (1993).
20. E. Kolbe, Phys. Rev. C **54**, 1741 (1996).
21. E. J. Moniz et al., Phys. Rev. Lett. **26**, 445 (1971).
22. Y. Fukuda et al., Phys. Rev. Lett. **81**, 1562 (1998).
23. L. A. Ahrens et al., Phys. Rev. D **35**, 785 (1987).
24. L. A. Ahrens et al., Phys. Lett. **B202**, 284 (1988).
25. L. A. Ahrens et al., Nucl. Inst. Meth. **A254**, 515 (1987).